Identification of *SOX3* as an XX male sex reversal gene in mice and humans

Edwina Sutton,[1] James Hughes,[1] Stefan White,[2] Ryohei Sekido,[3] Jacqueline Tan,[2] Valerie Arboleda,[4] Nicholas Rogers,[1] Kevin Knower,[5] Lynn Rowley,[2] Helen Eyre,[6] Karine Rizzoti,[3] Dale McAninch,[1] Joao Goncalves,[7] Jennie Slee,[8] Erin Turbitt,[2] Damien Bruno,[2] Henrik Bengtsson,[9] Vincent Harley,[5] Eric Vilain,[4] Andrew Sinclair,[2] Robin Lovell-Badge,[3] and Paul Thomas[1]

[1]School of Molecular and Biomedical Science and Australian Research Council Special Research Centre for the Molecular Genetics of Development, University of Adelaide, Adelaide, South Australia, Australia. [2]Murdoch Children's Research Institute and Department of Paediatrics, University of Melbourne, Royal Children's Hospital, Melbourne, Victoria, Australia. [3]Division of Developmental Genetics, MRC National Institute for Medical Research, London, United Kingdom. [4]Department of Human Genetics, David Geffen School of Medicine, UCLA, Los Angeles, California USA. [5]Prince Henry's Institute of Medical Research, Melbourne, Victoria, Australia. [6]Women's and Children's Hospital, North Adelaide, South Australia, Australia. [7]Centro de Genética Humana, Instituto Nacional de Saúde Dr Ricardo Jorge, Lisbon, Portugal. [8]Genetic Services of Western Australia, King Edward Memorial Hospital, Subiaco, Western Australia, Australia. [9]Department of Statistics, University of California, Berkeley, California, USA.

Sex in mammals is genetically determined and is defined at the cellular level by sex chromosome complement (XY males and XX females). The Y chromosome–linked gene sex-determining region Y (*SRY*) is believed to be the master initiator of male sex determination in almost all eutherian and metatherian mammals, functioning to upregulate expression of its direct target gene *Sry*-related HMG box–containing gene 9 (*SOX9*). Data suggest that *SRY* evolved from *SOX3*, although there is no direct functional evidence to support this hypothesis. Indeed, loss-of-function mutations in *SOX3* do not affect sex determination in mice or humans. To further investigate Sox3 function in vivo, we generated transgenic mice overexpressing *Sox3*. Here, we report that in one of these transgenic lines, *Sox3* was ectopically expressed in the bipotential gonad and that this led to frequent complete XX male sex reversal. Further analysis indicated that Sox3 induced testis differentiation in this particular line of mice by upregulating expression of *Sox9* via a similar mechanism to Sry. Importantly, we also identified genomic rearrangements within the *SOX3* regulatory region in three patients with XX male sex reversal. Together, these data suggest that SOX3 and SRY are functionally interchangeable in sex determination and support the notion that *SRY* evolved from *SOX3* via a regulatory mutation that led to its de novo expression in the early gonad.

Introduction

Sex in mammals is genetically determined and is defined at the cellular level by sex chromosome complement (XY males and XX females) and at the phenotypic level by the development of gender-specific anatomy, physiology, and behavior. Disorders of sexual development (DSDs) in humans are characterized by a complete or partial mismatch between genetic sex and phenotypic sex. Collectively, DSDs occur in at least 1 in 100 live births (1) and include relatively mild forms such as hypospadias (1 in 500 births) as well as more severe conditions such as ambiguous genitalia (1 in 4,500 births) and complete sex reversal (46, XY females and 46, XX males; 1 in 20,000 births). Although the etiology of many DSDs is not known, some cases of complete XX male and XY female sex reversal are associated with translocations or mutations of the Y-linked testis-determining gene *SRY* (sex-determining region Y) (2–8). *SRY* encodes a transcription factor that contains a highly conserved high-mobility group (HMG) DNA-binding domain and poorly conserved N- and C-terminal domains. Gain-of-function and loss-of-function studies in mice have demonstrated that *Sry* is necessary and sufficient for testis development (4, 7). Indeed, except in two species of the vole *Ellobius* (9) and the spiny rat (10), which lack the gene, *SRY* is believed to function as the master regulator of male sex determination in all therian (non-egg-laying) mammals (11).

The gonads develop from a band of mesoderm, the genital ridge (GR), that lies ventrally subjacent to the mesonephros, and together these constitute the urogenital ridge. The GR is considered to be bipotential, as it contains precursors that can differentiate into testis- or ovary-specific cell lineages (12). In mice, *Sry* is expressed in a transient center-to-pole wave in the XY GR from approximately 10.5 to 12.5 dpc (13, 14). Analysis of hypomorphic *Sry* alleles and inducible *Sry* transgenic mice indicate that the level of Sry activity must exceed a critical threshold within a developmental window of approximately 6 hours (12–15 tail somite [ts] stage) for irreversible commitment to a male fate (15–17). Despite its pivotal role in directing male differentiation, it appears that the sole critical function of Sry in sex determination is to upregulate its direct target gene *Sox9* (*Sry*-related HMG box–containing gene 9), thereby initiating Sertoli cell differentiation (18–20). Sertoli cells subsequently undergo a period of rapid proliferation, aided by Sox9/Fgf9 and Sox9/Pgd2 positive feedback loops (21, 22), and migrate and surround germ cells within the gonad to form testis cords. Sertoli cells also drive the male-specific migration of cells from the underlying mesonephros into the gonad. These are mostly endothelial cells that give rise to the coelomic vessel and other testis-specific vasculature (23). By 12.5 dpc, steroidogenic Leydig cells have differentiated and, just 48 hours after Sry begins to initiate the male pathway, the early testis already has a highly organized stereotypical structure and is morphologically distinct from the ovary, which remains a mass of germ cells scattered within the gonadal mesenchyme.

Although female development has traditionally been considered by some to be a "default" pathway, it is now clear that sexual fate is determined by a balance of opposing signals within the gonad, in which *Sry* exerts a dominant masculinizing influence (22, 24). For example, loss-of-function mutations in *Wnt4* and *Rspo1* cause partial XX male sex reversal, indicating that canonical Wnt signaling

Conflict of interest: The authors have declared that no conflict of interest exists.
Citation for this article: *J Clin Invest.* 2011;121(1):328–341. doi:10.1172/JCI42580.

predisposes the gonad to an ovarian fate (22, 25–29). Furthermore, gain-of-function mutations in *Wnt4* and *Ctnnb1* induce XY female sex reversal. While it is possible that high levels of pro-ovarian signals could block *Sry* activity, the evidence so far suggests that the effect of high levels of β-catenin is to prevent the maintenance of *Sox9* expression (27, 29, 30). Unexplained cases of *SRY*-negative XX male sex reversal in humans may therefore arise from loss-of-function mutations in members of the pro-ovarian pathway (such as canonical Wnt signaling components) or gain-of-function mutations in genes that mimic *SRY* activity, of which members of the *SOX* gene family are good candidates.

SRY-related HMG box–containing gene 3 (*SOX3*) is a single-exon gene located in a highly conserved region of the X chromosome in therian mammals (31–33). Other vertebrate species also possess homologs of *SOX3*, but none of these have been found to be sex-linked, even in prototherian mammals, such as the echidna (34). Of the 20 *SOX* genes in the mammalian genome, *SOX3* encodes a protein that is most similar to SRY, sharing 67% amino acid identity (and 90% similarity) across the DNA-binding HMG domain (31, 35). Comparative sequence data, coupled with molecular and cytogenetic studies of sex chromosomes, have led to the hypothesis that *SRY* arose during early mammalian evolution from a gain-of-function mutation in the proto-Y allele of *SOX3*. This mutation is thought to have activated gonadal expression of the proto-Y *SOX3* allele, resulting in the emergence of a novel sex determination switch that is specific to therian mammals (32, 36). Consistent with this hypothesis, *Sox3* expression is exceedingly low or absent in the developing gonads of mice and marsupials (33, 37). *Sox3* is, however, widely expressed in the central nervous system of vertebrate embryos and is required for normal brain development and function in mice and humans, as well as in pituitary and craniofacial development (31, 38–44). Importantly, mice and humans with mutations in *SOX3* do not show any defects in sex determination, although postnatal differentiation of some spermatogonia and the survival of some follicles are affected in *Sox3*-null mice (40, 45, 46). Thus, although *SOX3* does not normally function in sex determination, the proposed evolutionary link between *SOX3* and *SRY* raises the intriguing possibility that certain gain-of-function mutations in *SOX3* may cause XX male sex reversal in mice and humans.

In addition to loss-of-function mutations of *SOX3*, duplications of the locus can also lead to pituitary hormone deficiencies in humans (38, 41, 47). This was assumed to be due to overexpression, and therefore, to investigate this further, transgenic mice were derived using a large mouse *Sox3* genomic fragment. Some of these mice developed CNS abnormalities (P. Thomas, unpublished observations). However, here we describe a transgenic model of complete XX male sex reversal in which *Sox3* is ectopically expressed in the developing XX gonads due to a position effect. Initiation of the testis pathway in XX hemizygous transgenic (Tg/+) gonads induced *Sox9* upregulation, Sertoli cell differentiation, testis cord formation, and generation of a male-specific vasculature. Cotransfection assays using the recently identified *Sox9* testis-specific enhancer element (TESCO; ref. 18) showed that SOX3, like SRY, had modest transactivation activity and functioned synergistically with steroidogenic factor–1 (SF1) in this context. Importantly, *Sox3* failed to induce XX testis development in gonads that lacked *Sox9*. We also present 3 patients with XX male sex reversal, each of which has a unique genomic rearrangement of the *SOX3* regulatory region. Together, these data suggest that Sox3 gain-of-function in the developing gonad induces testis development by functioning as a surrogate for Sry. Our findings also provide important functional evidence to support the long-standing hypothesis that *Sox3* is the evolutionary precursor of *Sry* and suggest that rearrangements of *SOX3* are a relatively frequent cause of XX male sex reversal in humans.

Results

Complete XX male sex reversal exhibited in a line of Sox3 transgenic mice. To investigate the developmental impact of *Sox3* overexpression, we generated transgenic mice using a 37-kb murine *Sox3* genomic fragment that included an IRES-EGFP reporter cassette. Intriguingly, 1 of 20 lines that we generated contained an excess of male progeny, suggesting XX male sex reversal. Comparison of genotype, chromosomal sex, and phenotypic sex of 670 weaned progeny revealed that XX male sex reversal had occurred in approximately 77% of XX hemizygous transgenic (Tg/+) animals. Accordingly, this transgenic line was named *Sox3* transgene *Sex reversed* [*Tg(Sox3)1Pqt*, abbreviated here to *Sr*]. XX Tg/+ males exhibited normal male external genitalia (Figure 1, A–C), with completely masculinized reproductive tracts (Figure 1, D–F; $n = 4$), although their testes were significantly smaller than those of XY males and lacked sperm (Figure 1, G–I). Transgenic animals exhibited normal male mounting behavior.

Sox3 Tg/+ XX gonads express Sox9 and activate the testis differentiation pathway. To investigate the mechanism of sex reversal in *Sr* mice, we analyzed gonad morphology and expression of male-specific marker genes at 13.5 dpc, when the outcome of sex determination is morphologically evident (Figure 2). Most XX Tg/+ gonads had a normal male appearance, including the presence of testis cords and a coelomic vessel extending across the ventral surface of the gonads (Figure 2A). Robust expression of *Sox9* and its direct target gene *Amh* (48) was also clearly evident in the testis cords (Figure 2A). Confocal analysis revealed that EGFP (which completely overlapped with Sox3, Supplemental Figure 1; supplemental material available online with this article; doi:10.1172/JCI42580DS1) was expressed in Sertoli cells (and some interstitial cells) but not germ cells (data not shown), consistent with a direct role for this *Sox3* transgene in Sertoli cell differentiation (Figure 2B). Interestingly, some XX Tg/+ gonads exhibited regionally localized/restricted expression of the *Sox3* transgene (Figure 3, A and B). In these cases, the location and intensity of expression from the transgene closely correlated with levels of Sox9 expression and the extent of testis cord formation. Moreover, this was always seen in the central and anterior regions of the gonad, consistent with other cases of ovotestis development and with these regions being the most sensitive to male-inducing signals (refs. 49, 50, and Figure 3). A small proportion (5 of 32) of 13.5-dpc XX Tg/+ gonads did not express detectable levels of the transgene, and this correlated with the absence of both *Sox9* expression and testis cord formation (data not shown). Taken together, these data demonstrate a strong correlation among transgene expression, *Sox9* activation, and testicular phenotype.

Sox3 from the Sr transgene mimics Sry in its early expression and function. Activation of *Sox9* expression in supporting cell precursors by Sry is normally required for their differentiation into Sertoli cells and subsequent testis development. However, Sox9 itself can induce testis differentiation when it is ectopically expressed in the early gonad or even in cases where the locus has been duplicated (51–53). This implies that *Sox9* is the only critical target of Sry but also raises the question as to whether Sox3, from the *Sr* transgene, acts like Sry

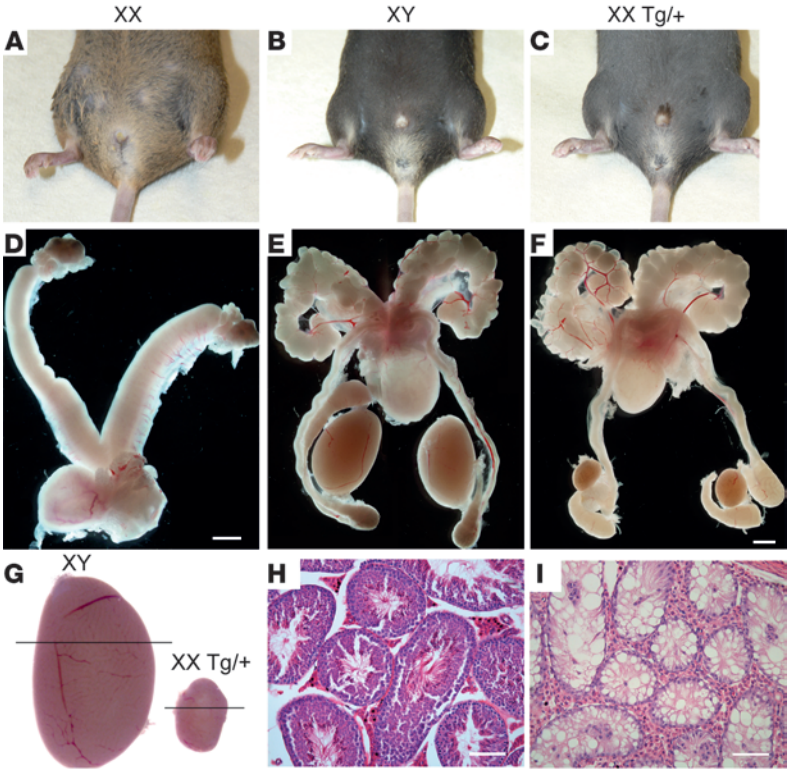

Figure 1
XX Tg/+ adults develop as males. (**A**–**C**) External genitalia of XX, XY, and XX Tg/+ individuals. Note the male phenotype of the XX Tg/+ animal. (**D**–**F**) XX, XY and XX Tg/+ internal reproductive tracts. Scale bars: 2 mm. (**G**) XY and XX Tg/+ testes. (**H** and **I**) Histological sections of XY and XX Tg/+ testes, respectively, showing the absence of sperm in the latter. Scale bars: 100 μm. All animals used for this analysis were between 20 and 24 weeks of age.

or Sox9. The former would be consistent with the higher degree of similarity between the HMG box domains of Sry and Sox3, while the latter might reflect the presence of strong transactivation domains at the C-termini of both Sox9 and Sox3 (although with little homology), whereas no such domain is found in Sry (18, 33).

To address this, it was important to first look at details of expression from the *Sox3 Sr* transgene (*Sox3-SrTg*). Endogenous Sry can first be detected at approximately 12 ts, and is shortly followed by an upregulation of Sox9 in Sry-positive cells (19). Expression of the *Sox3* transgene was also first detected at 12 ts (see below), and by 13 ts, several Sox3-positive cells were clearly present in the XX Tg/+ GR (Figure 4A). Some of these were also Sox9-positive (arrows), suggesting that Sox3 is directly involved in activating *Sox9* expression in the XX Tg/+ GR. XY GRs had a similar small number of Sox9-positive cells, reflecting the initial upregulation of Sox9 by Sry (Figure 4A). Consistent with their differentiation along the testis pathway, and similar to control XY gonads, XX Tg/+ GRs exhibited robust Sox9 expression at 19 ts (approximately 11.5 dpc), and this regionally coincided with EGFP expression across the GR (Figure 4B and data not shown). High-magnification confocal analysis revealed coexpression of EGFP and Sox9 consistent with cell autonomous induction of *Sox9* by Sox3. There was not an exact correlation, however, as EGFP-positive, Sox9-negative cells were also observed in 11.5-dpc and 12.5-dpc XX Tg/+ gonads (Figure 4B and data not shown). These may represent cells fated to be Sertoli cells that have yet to upregulate Sox9, or interstitial cell precursors. We also found some Sox9-positive, EGFP-negative cells in the XX Tg/+ genital ridges (Figure 4B). These probably represent supporting cell precursors recruited to the Sertoli lineage by preexisting Sertoli cells, which occurs in early XY gonads via non-cell-autonomous mechanisms (21, 22).

Sox3, like Sry, transactivates the Sox9 testis-specific enhancer element TESCO through synergistic interaction with Sf1. Sry upregulates *Sox9* transcription in the testis through binding and activation of a gonad-specific enhancer, testis-specific enhancer of *Sox9* (TES), synergistically with Sf1 (18, 54). To further investigate functional similarity of Sox3 and Sry, we performed transactivation assays in vitro using the TES core element (TESCO) (18). Consistent with previously published data, Sry activated TESCO, but only when Sf1 was coexpressed (Figure 4C and ref. 18). In the absence of Sf1, Sox3 also failed to transactivate TESCO. However, cotransfection of Sox3 and Sf1 resulted in approximately 2-fold activation above Sf1 alone, indicating that Sox3, like Sry, synergistically activates the TESCO enhancer, albeit to a slightly lesser degree (ref. 18 and Figure 4C). In contrast, greater than 14-fold activation of the TESCO reporter was detected when Sox9 and Sf1 were coexpressed compared with Sf1 alone. These results are also consistent with Sox3 acting like Sry, and not like Sox9, in this context.

Sox3 from the Sr transgene requires endogenous Sox9 to induce testes. To further explore whether Sox3 is acting exclusively like Sry, or whether it also mimics Sox9 function, we designed a genetic experiment to test if the *Sox3-SrTg* was able to induce sex reversal in the absence of *Sox9*. If Sox3 is functionally equivalent to Sry, the *Sox3-SrTg* should be unable to rescue or induce testis development in either XY or XX embryos also null mutant for *Sox9*. Conversely, if Sox3 acts like Sox9, the *Sox3-SrTg* should be able to substitute for both *Sry* and *Sox9* to promote testis cord formation. *Sox3-SrTg;Sox9$^{fl/fl}$;R26-Cre^{ERT2}* stud males were bred to *Sox9$^{fl/fl}$* females. Pregnant females were given tamoxifen at 9.5 and 10.5 dpc, a protocol found to give efficient Cre-mediated deletion of *Sox9* and XY female sex reversal (data not shown), or ethanol as a vehicle control, and embryos harvested at 12.5 dpc to determine genotype and gonadal phenotype. In some experiments, a *Tesco-cfp* transgene was included, to allow a simple assay of Sertoli cell differentiation (18). When tamoxifen was omitted, the *Sr* transgene was able to give XX male development, despite the altered genetic background (see below). However, after tamoxifen administration, we obtained 2 XY *Sox3-SrTg;Sox9$^{fl/fl}$;R26-Cre^{ERT2}* embryos, one with ovotestes and the other with morphologically normal ovaries, and a total of 6 XX *Sox3-SrTg;Sox9$^{fl/fl}$;R26-Cre^{ERT2}* embryos (4 with Tesco-cfp, 2 without), all of which had gonads with the morphological appearance of ovaries (Figure 5). Marker analysis revealed robust expression of Foxl2, which is specific to ovarian cell types (Figure 5). A number of Sox9-positive cells were still present due to inefficient action of tamoxifen in the embryos (data not shown), and these are likely to be the same cells that show relatively high levels

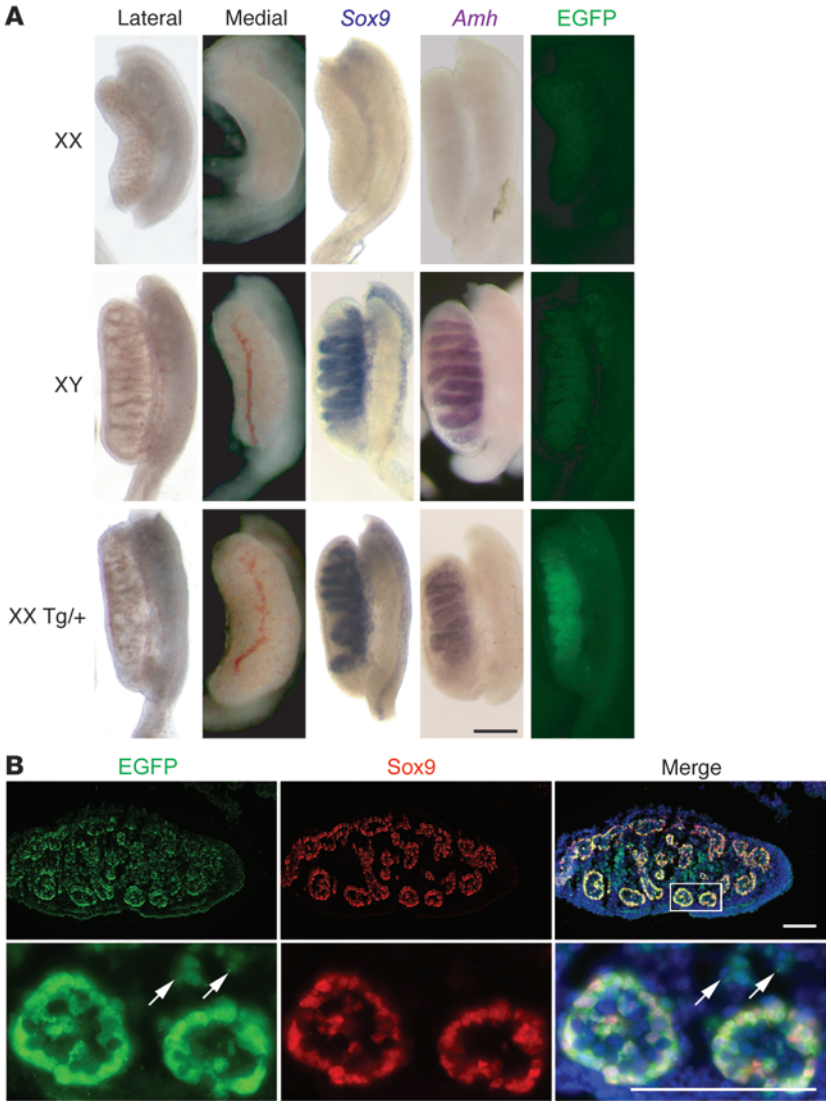

Figure 2
XX Tg/+ gonads have a normal male appearance and express the *Sox3* transgene at 13.5 dpc. (**A**) XX, XY, and XX Tg/+ 13.5-dpc gonads shown in lateral and medial views and analyzed for *Sox9* and *Amh* expression and EGFP fluorescence in unfixed tissue. Scale bar: 250 μm. (**B**) XX Tg/+ 13.5-dpc gonad section stained with EGFP and Sox9 antibodies. Lower panel shows higher-magnification view of the boxed region. Arrows indicate EGFP-positive, Sox9-negative cells in the interstitium. Scale bars: 50 μm.

of EGFP expression from the *Sox3-SrTg*. However, these were not present in sufficient numbers to have organized into testis cords or to have induced the testis-specific vasculature (Figure 5 and data not shown). Collectively, these results provide strong evidence that Sox3 from the transgene is not able to compensate for the loss of *Sox9*, and therefore that it behaves like Sry and not like Sox9.

Integration of Sr transgene upstream of the embryonic testis gene Aldh1a1. Sex ratios are unaffected in *Sox3*-null mice, indicating that *Sox3* is not required for sex determination (40, 45). Furthermore, although very low levels of *Sox3* transcripts in 11.5-dpc gonads have been reported (33), we were unable to detect Sox3 protein in wild-type GRs during sex determination (data not shown). We therefore postulated that *Sox3* was ectopically upregulated in the gonads of *Sr* Tg/+ embryos due to a position effect. This was supported by analysis of a second independent *Sox3* transgenic line in which transgene expression was not detected in the gonads by immunohistochemistry (11.5 dpc and 13.5 dpc) or quantitative RT-PCR (qRT-PCR) (11.5 dpc) despite comparable CNS expression (data not shown). Furthermore, none of 8 XX *Sox3* transgenic founders that were generated exhibited XX male sex reversal (data not shown). We initially characterized the *Sr* integration site using FISH analysis of metaphase chromosomes, which revealed a single transgene insertion site on chromosome 19 in the B/C1 region (Figure 6B). GenomeWalker, PCR, and Southern blot analyses confirmed these data and revealed that 2 copies of the transgene construct had integrated upstream of the retinaldehyde dehydrogenase A1 (*Aldh1a1*, also known as *Raldh1*) gene (Figure 6, A, C, and D, and data not shown). The *Aldh1a1* gene product Aldh1a1 catalyzes the conversion of retinaldehyde into all-*trans*-retinoic acid, albeit with less efficiency than the related enzymes Aldh1a2 and Aldh1a3 (55, 56). Although not required for sex determination (57, 58), *Aldh1a1* was previously identified as a testis-enriched gene in a subtractive hybridization screen (59) and is strongly expressed in Sertoli cells and a subset of interstitial cells from 11.5 dpc onward (60). To assess whether *Aldh1a1* is upregulated during differentiation of XX Tg/+ gonads into testes, we compared *Aldh1a1* and *Sox9* expression during gonad differentiation by qRT-PCR (Figure 7A). At 13.5 dpc, *Aldh1a1* and *Sox9* expression was considerably higher in XX Tg/+ gonads compared with XX controls. However, expression of both genes was even higher in XY controls, at 13.5 dpc and 12.5 dpc, which suggests that activation of the male pathway is less efficient in the XX Tg/+ gonads, consistent with occasional ovotestis or ovary development (Figures 2 and 3). In situ hybridization and immunohistochemistry on 13.5-dpc gonads confirmed that *Aldh1a1* was strongly expressed in XX Tg/+ gonads, where it was localized to Sertoli and some interstitial cells in an identical pattern to XY controls (Figure 7, B–D, and data not shown).

Coexpression of Sox3 transgene and Aldh1a1 in Sertoli cells in XX Tg/+ gonads. To investigate whether proximity of the transgene to *Aldh1a1* could influence its expression, we compared the distribution of their gene products in XX Tg/+ gonads. At 13.5 dpc, we observed extensive overlap of Sox3 and Aldh1a1 throughout the gonad (Figure 7, C and D), including the Sertoli cells lining the testis cords, suggesting that regulatory elements from *Aldh1a1* may be important for ectopic transgene expression in the testis (arrows, Figure 7D). To further investigate the relationship between *Aldh1a1* and transgene expression during sex determination in XX Tg/+ gonads, we compared the distribution of Aldh1a1 and EGFP from 6 to 17 ts (Figure 8). Initially, Aldh1a1 was detected in the GR at very low levels, and no EGFP was present. By 12 ts, Aldh1a1-positive cells,

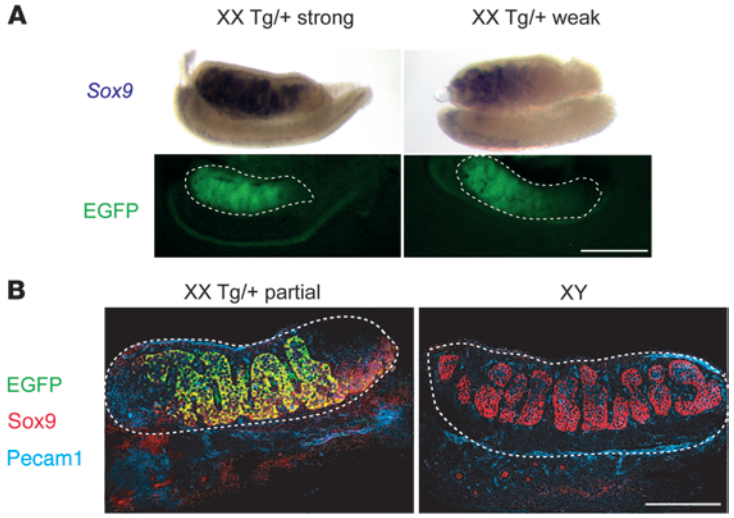

Figure 3
13.5-dpc XX Tg/+ gonads show variable cord formation and *Sox9* expression that coincides with the spatial localization of transgene (EGFP) expression. (**A**) *Sox9* expression and corresponding EGFP expression in representative XX Tg/+ (strong), and XX Tg/+ (weak) 13.5-dpc gonads. Scale bar: 250 μm. (**B**) Optical slices of whole mount 12.5-dpc XX Tg/+ and XY gonads stained with EGFP (green), Sox9 (red), and Pecam1 (blue). The dotted lines indicate the outline of the gonads. Scale bar: 150 μm.

detectable by in situ hybridization and immunohistochemistry, contained the initial population of EGFP-positive cells (Figure 8, box 1). By 17 ts, the number of EGFP-positive cells increased markedly, and most, if not all, of these cells also expressed Aldh1a1, albeit at low levels in some cases (Figure 8, box 2). The lack of clear singly positive EGFP cells suggests that *Aldh1a1* expression may provide a permissive regulatory environment for transgene activation. Once *Sox3* transgene expression is initiated in uncommitted XX gonads and *Sox9* expression is upregulated, a positive feedback loop may arise, resulting in robust coexpression of the transgene and Aldh1a1 in Sertoli cells (60).

Rearrangements of the SOX3 regulatory region are associated with XX male sex reversal in humans. Given that SOX3 function in the CNS is broadly conserved in mice and humans and that *Sox3* is able to induce sex reversal when ectopically expressed in the developing murine GR, it is possible that rearrangements at the *SOX3* locus are associated with human XX male sex reversal. We therefore screened a cohort of 16 *SRY*-negative 46, XX male patients for copy number variation using Affymetrix 6.0 whole genome SNP (7 patients) and Illumina 1M (9 patients) microarrays. Rearrangements covering or in close proximity to *SOX3* were identified in 3 patients (Figure 9, Supplemental Figures 2 and 3, and Table 1). Patient A contained two microduplications of approximately 123 kb and 85 kb, the former of which spanned the entire *SOX3* gene. Previously published examples of *SOX3* duplications in 46, XY males have been associated with pituitary hormone deficiencies and cognitive defects, whereas 46, XX female carriers have been unaffected (38, 47). Consistent with these data, there was no evidence of hypopituitarism or intellectual disability in this patient. X-inactivation studies showed no evidence for skewed inactivation in DNA derived from lymphocytes (data not shown). FISH analysis using a BAC clone covering the *SOX3* gene consistently gave a stronger signal on one of the X chromosomes, indicative of tandem duplication (Supplemental Figure 3). The centromeric duplication is approximately 70 kb downstream from the *SOX3* gene, very close to a previously described deletion-insertion breakpoint in individuals with X-linked hypoparathyroidism (61), which was postulated to have a positional effect on *SOX3* expression. Patient B contained a single 343-kb microdeletion immediately upstream of *SOX3*. Unlike in patient A, the coding sequence of *SOX3* is not affected in this patient, suggesting that altered regulation (and not increased dosage) of *SOX3* is the cause of XX male sex reversal. Patient C has a more complex phenotype that also includes a scrotal hypoplasia, microcephaly, developmental delay, and growth retardation. This patient has a large (approximately 6-Mb) duplication that encompasses *SOX3* and at least 18 additional distally located genes, overexpression of which probably contributes to the phenotypic complexity. Notably, the proximal breakpoint falls within the *SOX3* regulatory region (62) and is close to the proximal *SOX3* duplication breakpoint in patient A (Figure 9).

To investigate the possible mechanism of sex reversal in these patients, we performed transactivation assays using a human *SOX9* testis enhancer sequence (hTES) that is homologous to the mouse TESCO element (18, 63). hSOX3 and hSRY activated hTES approximately 10- and 5-fold, respectively. Activation levels by these proteins were further enhanced in the presence of exogenous SF1, suggesting synergistic activation, similar to the murine system (Figure 10). Together, these data suggest that *SOX3* gain of function in humans can cause XX male sex reversal.

Discussion

Through characterization of a unique transgenic mouse line, we show that ectopic expression of *Sox3* in uncommitted XX gonads is sufficient to divert the program of ovarian development toward testis formation, leading to XX males. Our data indicate that Sox3 functions as a molecular switch, activating the testis differentiation pathway via a mechanism that is functionally analogous to Sry. Furthermore, we provide the first evidence to our knowledge that *SOX3* gain of function in humans can also lead to complete XX male sex reversal. Together, these data provide insight into the genetic mechanism of mammalian sex determination, the evolution of Sry, and the molecular pathology of disorders of sexual development.

Sox3 can function as an analog of Sry. Molecular genetic studies carried out mostly in mice and humans, but supported by work in other species, provide strong evidence that mammalian testis differentiation is critically dependent on a threshold of SOX9 activity in supporting cell precursors that, once exceeded, suppresses the pro-ovarian differentiation program and promotes and then reinforces Sertoli cell and subsequent testis differentiation (24, 53, 64). As shown in mice, Sry along with its cofactor Sf1 bind the TESCO enhancer element upstream of *Sox9* to mediate its initial upregulation (18). Based on the high sequence similarity

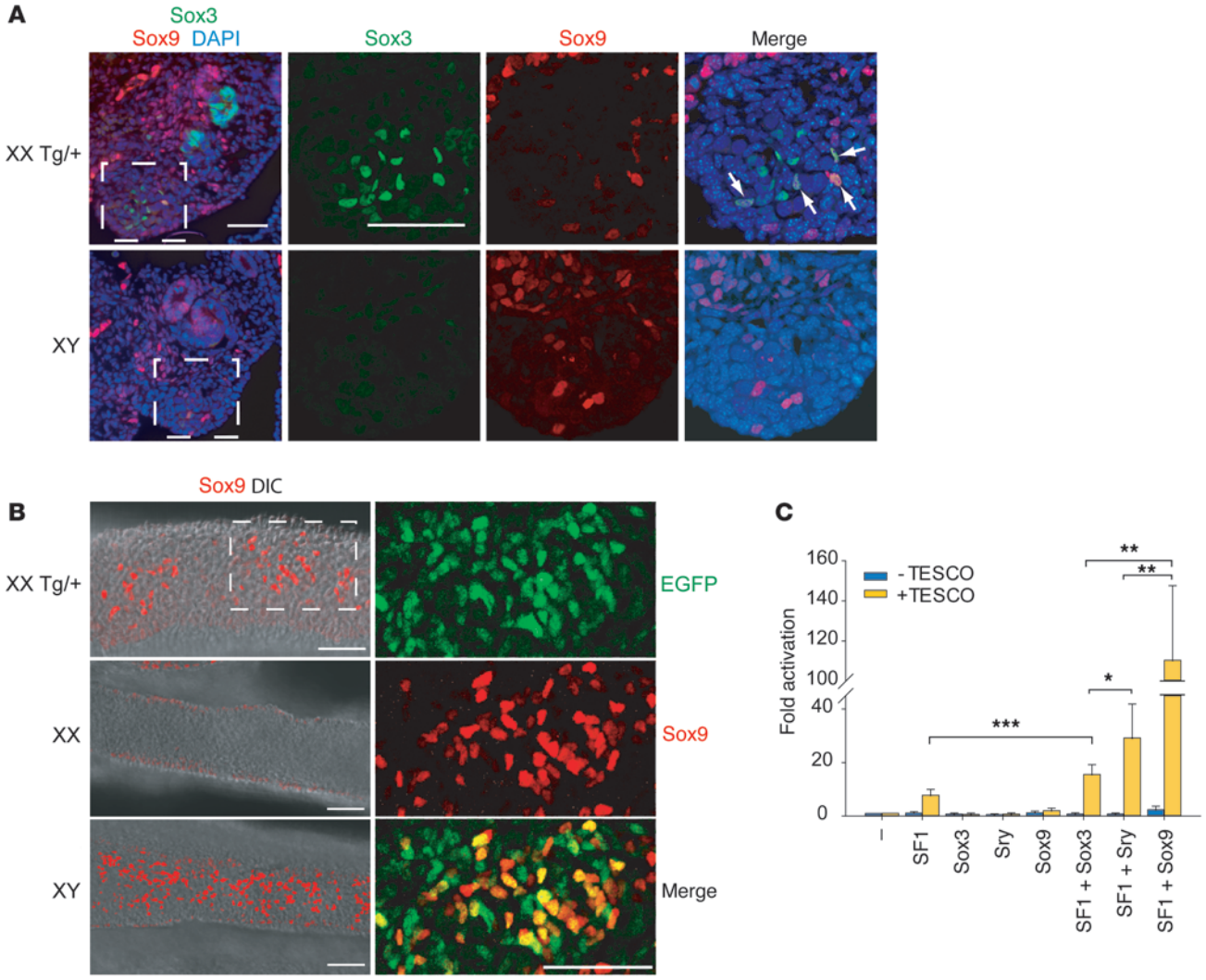

Figure 4

Mechanism of transgene-induced sex reversal and its activation in the gonads. (**A**) 13 ts XX Tg/+ and XY transverse sections presented as a 6-μm stack stained with Sox3 and Sox9. Enlargements corresponding to the boxed region are shown on the right. Arrows indicate Sox3/Sox9-positive cells. Scale bars: 50 μm. (**B**) Single optical slices of whole mount 11.5-dpc XX, XY, and XX Tg/+ genital ridges stained with Sox9 and presented as an overlay with corresponding differential interference contrast (DIC) image. Higher-magnification view of the boxed region in the XX Tg/+ genital ridge is shown in the right panel, presented as a 60-μm stack of optical sections and highlighting the extent of colocalization between Sox3 and Sox9. Scale bars: 50 μm. In **B**, genital ridges are oriented so that anterior is to the left and the coelomic epithelium at the top. (**C**) Transactivation experiment using the mouse *Sox9* TESCO enhancer reporter. Note that Sox3 and Sry exhibit similar synergistic activation of the reporter with SF1, but fail to activate in the absence of SF1. Negative control transfections using a reporter lacking the enhancer are also shown (–TESCO). Western blot analysis indicated that comparable levels of Sox3, Sry, and Sox9 protein were expressed (data not shown). Data are mean ± SEM. ***$P < 0.001$, **$P < 0.01$, *$P < 0.05$.

of Sox3 and Sry across the HMG domain and the proposed common evolutionary ancestry of their cognate genes (32), we hypothesized that Sox3 causes XX male sex reversal in *Sox3-SrTg* mice by functioning as a surrogate for Sry. Our data provide several lines of evidence to support this view. First, adult *Sr* XX males exhibit complete sex reversal and in this respect are phenotypically identical to XX *Sry* transgenic adult males (7). Second, both mouse and human SOX3 exhibit in vitro transactivation properties very similar to those of Sry on TESCO and its human equivalent, including a requirement for Sf1. These are rather weak in contrast to the strong activation shown by Sox9. While a strong transactivation domain at the C-terminus of Sox3 can be demonstrated in other contexts (38), this appears not to operate in the cotransfection assays reported here. Presumably this is because any interaction with Sf1, which could be via the HMG box of Sox3 (and Sry), is not sufficient to elicit further recruitment of transcriptional coactivators to the complex bound to TESCO. If there are no specific requirements for features other than the HMG box, then this would provide an explanation for the rapid drift in the non-box sequences of SRY during evolution (see below and ref. 64). Third, there is a close correlation between expression of the *Sox3* transgene and endogenous *Sox9* in the developing XX *Sox3-SrTg/+* gonad, suggesting that Sox3 may activate *Sox9* expression in vivo. Although a small proportion of Sox9-positive cells do not

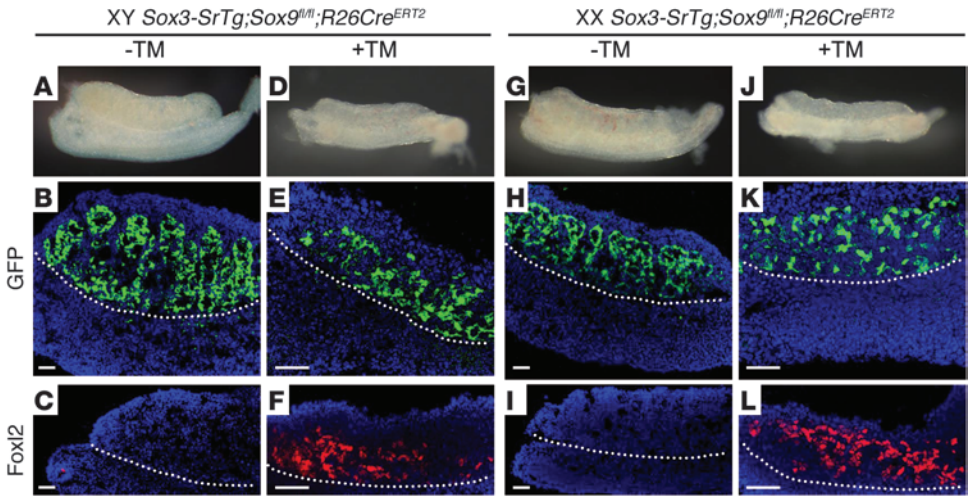

Figure 5
The *Sox3* transgene is not able to mimic *Sox9* in the gonad at 12.5 dpc. (**A**–**F**) XY *Sox3-SrTg;Sox9*$^{fl/fl}$*;R26Cre*^{ERT2} mice were either treated or not treated with tamoxifen (TM). In the absence of TM, the gonad developed into a normal testis containing testis cords (**A**–**C**). When *Sox9* was ablated after TM treatment, testis cords were not formed (**D** and **E**), and Foxl2-positive cells were detected in the gonad (**F**). (**G**–**L**) Similar experiments were performed for XX *Sox3-SrTg;Sox9*$^{fl/fl}$*;R26Cre*^{ERT2} mice. The mice developed XX sex-reversed testis without TM (**G**–**I**). In contrast, TM treatment resulted in ovarian morphology and the expression of Foxl2 (**J**–**L**). Scale bars: 0.5 mm (**A**, **D**, **G**, and **J**) and 50 μm (**B**, **C**, **E**, **F**, **H**, **I**, **K**, and **L**).

express the transgene during early XX Tg/+ gonadogenesis, this is reminiscent of Sox9-positive/Sry-negative cells that have been identified in XY gonads at the same stage, which arise through prostaglandin D2 and Fgf signaling (21, 22), suggesting that non-cell-autonomous recruitment of cells to the Sertoli lineage also occurs in XX Tg/+ gonads. Indeed, this might be expected if the *Sr* transgene corresponds to a slightly weak allele of *Sry*. Fourth, the *Sox3* transgene is expressed in the central gonad from 12 ts (Figures 4 and 8) and is therefore in the correct spatiotemporal location to influence the decision of the supporting cell precursors to adopt a male fate (16, 19, 65). Finally, we find that the *Sr* transgene also mimics *Sry* in vivo, because it depends on the presence of *Sox9* to trigger testis development. This again supports the notion that Sox3 from the transgene acts like Sry and not Sox9.

In contrast to *Sry*, transgene expression in the gonads of the *Sr* line is maintained in Sertoli cells beyond the critical window of sex determination. This is not surprising given that *Sry* is switched off once Sox9 reaches the critical threshold to trigger Sertoli cell differentiation, and it is unlikely that *Sox3* would respond in the same way (66, 67). Instead, *Sox3* expression may be maintained by virtue of its integration next to *Aldh1a1*, which itself is activated directly or indirectly by Sox9 (see below). The functional consequence of persistent transgene expression is not clear. Sox3 could activate multiple male-specific target genes, in a manner that is analogous to the promotion of male development by Sox9, although this possibility is not supported by the failure of the *Sr* transgene to elicit testis development in the absence of *Sox9*. Alternatively, by virtue of its relatively poor transactivation activity in this context (compared with Sox9), Sox3 could interfere with Sox9 action through competitive binding to its target sites, including to the TESCO enhancer. However, although *Sry* expression is normally turned off, this is not essential, as shown with a constitutively active *Sry* transgene, and it naturally stays on for an extended period in some species (65, 68). The continuous expression of Sox3 may therefore have little or no impact on subsequent testis development.

Delayed testis development and incompletely penetrant sex reversal in Sr transgenic XX gonads. While most *Sr* XX transgenic adults showed complete female-to-male sex reversal (77%), the gonadal development

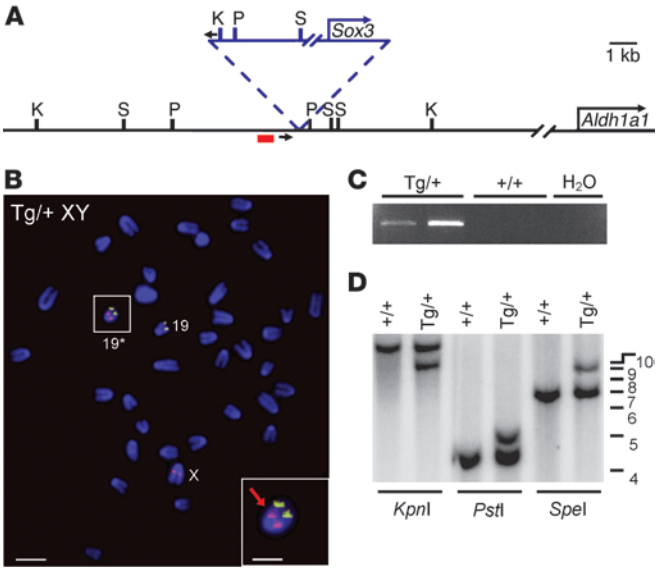

Figure 6
The *Sr* transgene has integrated upstream of *Aldh1a1* on chromosome 19. (**A**) Schematic representation of transgene insertion site on chromosome 19 illustrating PCR primer position (black arrows), Southern probe (red), and relevant restriction sites. (**B**) FISH analysis of Tg/+ XY metaphase chromosomes. *Sox3* transgene (modified RP23-174O19 BAC) and chromosome 19 (RP23-142D22 BAC) signals are shown in red and green, respectively. The inset shows a magnified view of chromosome 19 into which the transgene has integrated (19*). Scale bars: 2.5 μm; 0.5 μm in inset. (**C**) PCR assay of genomic DNA using primers that flank the transgene integration site. Product is amplified from Tg/+ DNA and not from +/+ DNA. All genomic DNA samples were shown to be amplifiable using *Gapdh* primers (data not shown). H_2O indicates negative control reaction. (**D**) Southern blot analysis comparing +/+ and Tg/+ DNA digested with *Kpn*I, *Pst*I, and *Spe*I. Marker sizes (kb) are shown on the right. Note the additional bands of expected size in each of the Tg/+ tracts. K, *Kpn*I; P, *Pst*I; S, *Spe*I.

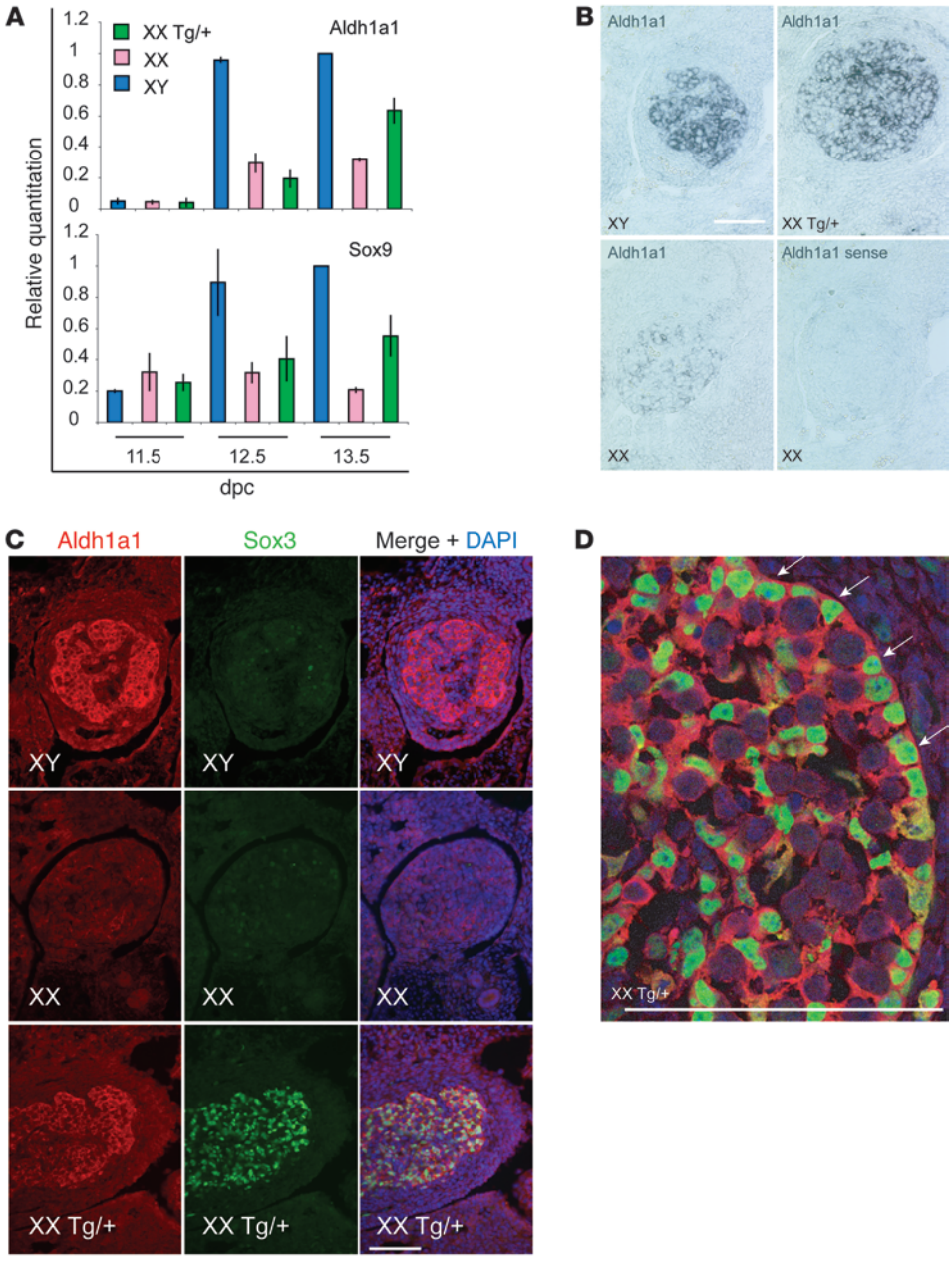

Figure 7
Expression profile of *Aldh1a1*/Aldh1a1 and Sox3 in XY and XX Tg/+ gonads from 11.5 to 13.5 dpc. (**A**) qRT-PCR analysis of 11.5- to 13.5-dpc gonads. Normalized expression levels of each gene are shown relative to β-actin. Two cDNA series were analyzed twice each, and error bars represent SD of the mean of the two series. (**B**) In situ hybridization showing *Aldh1a1* expression in transverse sections of 13.5-dpc XY, XX Tg/+, and XX gonads. No signal was detected using an *Aldh1a1* sense probe. (**C**) Transverse sections of XY, XX Tg/+, and XX 13.5-dpc gonads stained with Aldh1a1, Sox3, and DAPI. Protein expression levels are consistent with the transcript expression analysis shown in **B**. (**D**) Confocal micrograph of 13.5-dpc XX Tg/+ gonad showing the extensive overlap in Sox3 and Aldh1a1 expression. Arrows indicate Sox3/Aldh1a1-positive cells lining the testis cords. Scale bars: 100 μm.

of XX Tg/+ embryos was often delayed compared with XY controls, as evidenced by lower *Sox9* and *Aldh1a1* expression, fewer Sox9-positive cells, and incomplete testis cord formation especially at the posterior poles (Figure 3). This phenomenon has also been observed with weak *Sry* alleles such as Y-POS, in which normal onset but lower levels of *Sry* expression and, in some cases, reduced efficacy of Sry isoforms leads to reduced *Sox9* expression, a delay in testis cord development, and XY sex reversal on a C57BL/6 (B6) background (17, 69–72). qRT-PCR analysis of *Sry* and *Sox3* transcript levels in 11.5-dpc XY and XX Tg/+ gonads, respectively, indicated that these genes are expressed at similar levels (data not shown), suggesting that expression level per se is not the primary cause of the developmental delay. A more likely explanation is that Sox3 is a less efficient activator of *Sox9*, given its weaker transactivation activity on the *Sox9* enhancer element TESCO in the presence of Sf1 (Figure 4). We also noticed that increased contribution of the pro-ovarian B6 genetic background (73) reduced the penetrance of sex reversal in the *Sr* line, resulting in XX Tg/+ gonads that lacked transgene expression completely (Supplemental Figure 4). One explanation for this might be the earlier and more robust pro-ovarian program in B6 gonads preventing the reinforcement of transgene expression and the male pathway (30, 70, 73). Thus, Sox3, like Sry, may function in a narrow window of competence so that any genetic or environmental conditions that reduce its capacity to reach the critical threshold required for Sertoli cell differentiation lead to delayed development of testes, to ovotestis, or even to ovaries.

Aldh1a1 and transgene regulation in the gonads. We were unable to detect Sox3 protein in the GR of wild-type XY or XX embryos, indicating that *Sox3* is ectopically expressed in *Sr* gonads. Furthermore, EGFP was not expressed in the GRs of an independent *Sox3* transgenic line (which does not exhibit XX male sex reversal), suggesting that regulatory elements flanking the *Sr* integration site control transgene expression in the gonad. Mapping studies indicated that the *Sr* transgene had inserted upstream of *Aldh1a1*, a gene with sexually dimorphic expression. *Aldh1a1* is expressed at much higher levels in embryonic testis in comparison with ovaries at 12.5 dpc and 13.5 dpc (ref. 60 and Figure 7), and in the former is restricted to Sertoli cells and an undefined population of interstitial cells. The overlap of Sox3 and Aldh1a1 expression in XX transgenic gonads at these time points suggests that regulatory elements associated

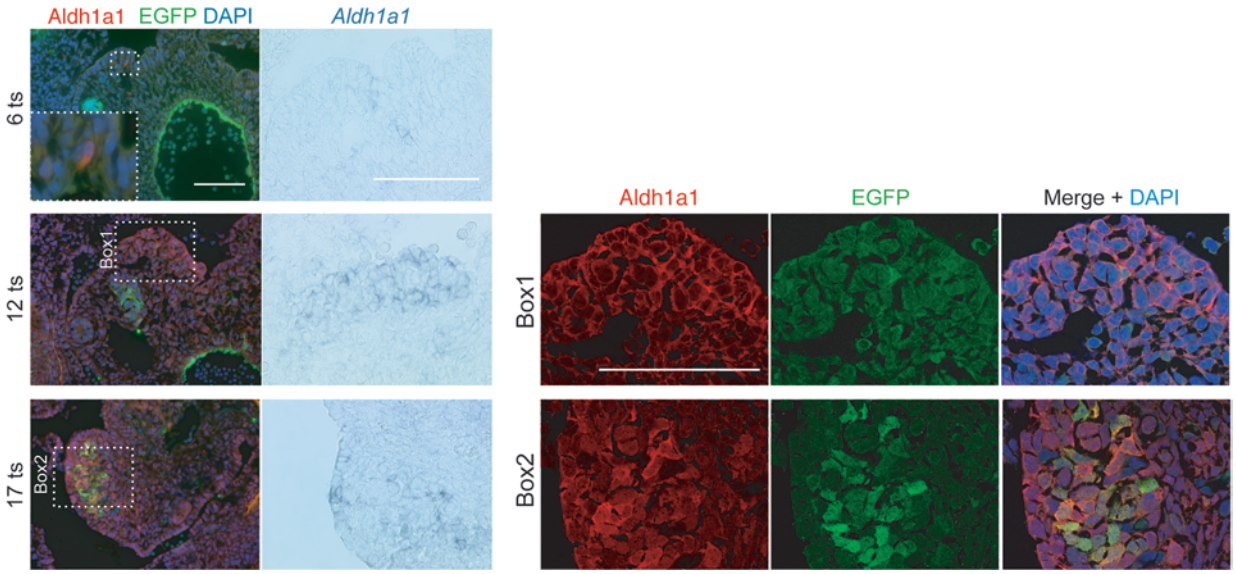

Figure 8
Expression of Aldh1a1 and EGFP in the gonadal ridge of XX Tg/+ gonads at 6–17 ts. Immunohistochemistry and in situ hybridization of serial transverse sections showing EGFP and Aldh1a1 distribution in 6–17 ts embryos. Given the low level of Aldh1a1 protein in the XX Tg/+ GR during these early stages of sex determination, the expression of *Aldh1a1* in adjacent sections is included at each stage for comparison. Aldh1a1/*Aldh1a1* is first observed at 6 ts (magnified in box inset). Aldh1a1/*Aldh1a1* is detected in a diffuse pattern at 12 ts. A rare EGFP-positive cell is found within a population of Aldh1a1-positive cells in the GR at this stage (magnified in box 1). At 17 ts, Aldh1a1/*Aldh1a1* becomes more restricted, while the abundance of EGFP within the GR increases (magnified in box 2). Scale bars: 100 μm.

with testis-specific expression of *Aldh1a1* may also control the *Sr* transgene. However, as discussed above, irreversible commitment to a male fate would almost certainly require transgene expression in the GR between 12 and 15 ts, prior to *Aldh1a1* expression becoming sexually dimorphic. Intriguingly, *Aldh1a1* and transgene expression overlap in XX Tg/+ gonads at 12–18 ts, although coexpression appears to be restricted to a subpopulation of Aldh1a1-expressing cells. These data suggest that transcriptional activity from *Aldh1a1* in the context of the bipotential XX Tg/+ gonad may create a permissive chromatin environment that is necessary but not sufficient for transgene activation. Perhaps the latter occurs only in cells expressing Sf1 or another factor restricted to supporting cell precursors. However, after transgenic XX gonads switch to a testis differentiation program, transgene expression (unlike *Sry*) is upregulated in Sertoli cells. While the regulatory element(s) that direct *Aldh1a1* expression are not known, a recent study indicates that *Aldh1a1* is genetically downstream of *Sox9* (60). This may have implications for the amplification and/or maintenance of *Sox3* expression in *Sr* gonads and provides a direct link to *Sox9*, not only in establishing the male pathway but also in regulating transgene expression. Identification of *Aldh1a1* gonadal enhancers may provide useful tools for transgenic analysis of gonad development and would likely lead to a better understanding of transgene regulation in *Sr* transgenic embryos.

Sox3, Sry, and the evolution of the mammalian sex determination switch. Comparative cytogenetic and sequence analyses indicate that the mammalian sex chromosomes evolved from a pair of autosomes, termed the proto-X/Y (36). It has been proposed that *Sry* was generated by a dominant mutation of the proto-Y *Sox3* allele in a mammalian ancestor approximately 200 million years ago, prior to divergence of the therian lineage (32, 36). The functional interchangeability of Sox3 and Sry demonstrated here indicates that their sole conserved domain, the HMG box, may be all that is critical for sex determination. This is in agreement with the (exclusive) conservation of the HMG domain in *SRY* genes, transgenic domain swap experiments in mice, and the predominance of *SRY* HMG mutations in XY females (35, 74, 75). The finding that Sox3 can promote male development when expressed in the genital ridge, in a manner that is comparable to Sry, adds further evidence against the hypothesis that Sox3 is required for ovary development or that Sry is a dominant negative version of Sox3, repressing the latter's activity (or expression) (76). Instead it implies that the evolution of *Sry* involved a mutation event that led to expression of one allele of *Sox3* (the proto-*Sry*) within the supporting cell lineage of the genital ridge. This mutation may have been subtle, with the proto-*Sry* retaining the conserved pattern of *Sox3* expression within the CNS and elsewhere, or it could have involved a deletion or translocation, where most of the latter was lost. In several species examined, including mouse, rat, and human, *Sry* is expressed in parts of the developing and adult CNS (77–79), although given the rapid evolution of *Sry* flanking sequences, it will be a challenge to prove whether this reflects conservation of specific regulatory elements or the acquisition of new ones. Concomitant with the change in proto-*Sry* expression, *Sox9* must have acquired the ability to respond to it. If, however, Sox9 was already involved in regulating its own expression within the Sertoli cell lineage of the therian ancestor, as shown in the mouse (18), then this capacity to respond to the proto-Sry may have already existed. To this end, recent evolutionary analyses have demonstrated that conserved elements within TESCO are present in all tetrapods, suggesting that mechanisms of *Sox9* regulation are conserved and precede the evolution of *Sry* (63).

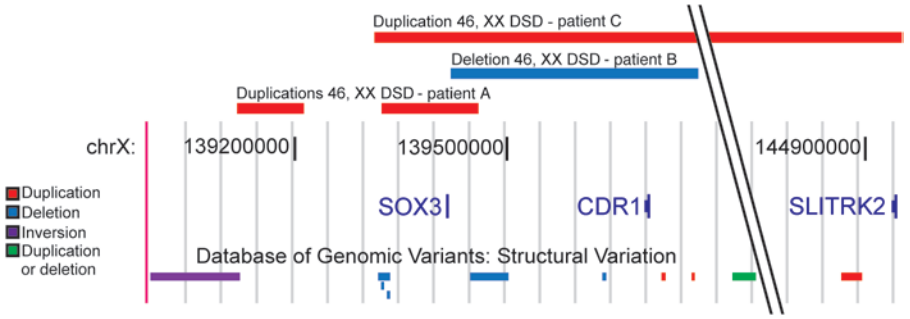

Figure 9
SOX3 rearrangements in 46, XX males. An image derived from the UCSC genome browser (http://genome.ucsc.edu) showing the location of the rearrangements identified in patients A–C in relation to the *SOX3* gene. Also shown are rearrangements previously identified in healthy individuals (as recorded in the Database of Genomic Variants; http://projects.tcag.ca/variation), including CNVs and an inversion. It is noteworthy that duplication breakpoints in patients A and C are in close proximity to other known CNV/inversion breakpoints, suggesting structural or sequence motifs that may be responsible for recurrent rearrangements. Numbering corresponds to nucleotide position on the X chromosome (chrX), based on reference sequence hg18.

SOX3 rearrangement is associated with XX male sex reversal in humans. Cases of *SRY*-negative XX male sex reversal are particularly intriguing, and their genetic basis has been debated extensively in the literature since *SRY* was identified almost 20 years ago. To date, loss of only one gene, *RSPO1*, has been shown to be associated with a clear XX male sex reversal condition, albeit in an unusual syndromic form of this disorder involving skin abnormalities (palmoplantar hyperkeratosis and predisposition to squamous cell carcinoma; ref. 26). Genomic rearrangements and mutations of *SOX9*, *SOX10*, and *SF1* have also been detected in rare cases of XX male and XY female sex reversal (80–82), although the molecular etiology of most cases is unknown. In this study, we have identified *SOX3* rearrangements in 3 patients with XX male sex reversal. Furthermore, we show that hSOX3 transactivates a human TES-like enhancer sequence, suggesting that human *SOX3*, like its murine counterpart, can functionally compensate for *SRY*. In contrast to the murine TESCO analysis, transactivation experiments using hTES were performed in CHO cells in which endogenous SF1 is already present. This is likely to function in synergy with hSOX3 and hSRY to give the observed limited transactivation in the absence of exogenous SF1 (82). Taken together, these data raise two possible mechanisms by which SOX3 could activate the male differentiation pathway in these patients: increased dosage or ectopic expression. Based on previous reports of *SOX3* duplication in humans (which is associated with hypopituitarism and variable mild intellectual disability; refs. 38, 47) and the absence

Table 1
Clinical summary of 46, XX male patients with *SOX3* rearrangements

	Patient A	Patient B	Patient C
Age at evaluation	30 yr	Endocrine: 19 yr; histology: 26 yr	19 mo
Height	165 cm	167.5 cm	75.2 cm
FSH[A]	22.0 mIU/ml	69.0 mIU/ml	
LH[B]	11.1 IU/L	35.0 IU/l	
Prolactin[C]	17.9 μg/l	3.0 μg/l	
Free testosterone[D]	1.92 ng/dl (early morning)	0.86 ng/dl (afternoon measurement)	
Testicular volume	~5 ml	~6 ml and soft	Right testicle appears smaller than left testicle
Penis size		Shaft length, 10.2 cm; shaft diameter, 2.6 cm	Shaft length, 3.4 cm
Genitals and testis		Histology: Atrophic changes with loss of normal spermatogenesis; thickening and hyalinization of the tubular basal lamina and diminished number of interstitial cells; normal spermatic cords	Hypoplastic scrotum; testes are retractile and can be brought down
Secondary sexual characteristics	Normal	Tanner stage 5 pubic hair and penile development with small testis; onset age, 13 yr	N/A
Developmental issues		Gender dysphoria from 6 years; referred to behavior therapist	Developmental delay; microcephaly; growth retardation

All units given in conventional units (defined in ref. 95). [A]FSH: male reference range 5–20 mIU/ml. [B]LH: male reference range, 5–20 IU/l. [C]Prolactin reference: 5–20 μg/l. [D]Normal male free testosterone, >6.5 ng/dl (96).

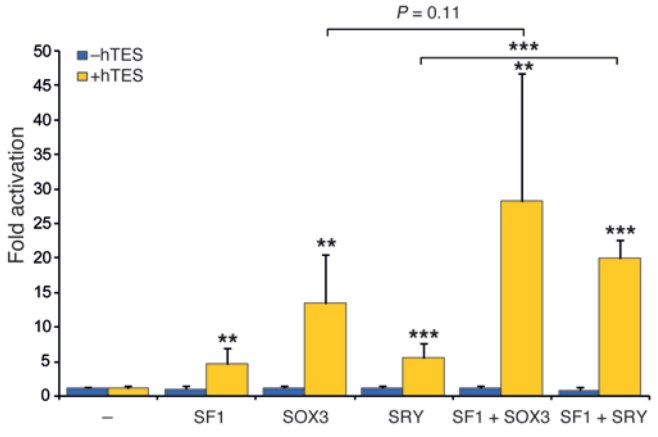

Figure 10
SOX3 activates the hTES. Human SOX3 (100 ng) activates hTES-*luc* (1.6 μg) (10–fold) compared with human SRY (100 ng) (5-fold) in CHO cells. In the presence of added SF1 (20 ng), further transactivation occurs with both SOX3 (25-fold) and SRY (20-fold) (n = 2–3). Error bars represent SD. Unless otherwise indicated, statistical comparisons were made between fold activations of expression vector and control empty vector. ***P < 0.001, **P < 0.01.

of Sox3 protein in murine bipotential gonads, it is unlikely that increased dosage of *SOX3* in these 3 patients is the mechanism responsible for the sex reversal. It is more probable that rearrangement of the *SOX3* locus, through duplication or deletion, leads to ectopic gonadal expression and subsequent activation of the male pathway at a critical stage of sex determination. As conserved elements that direct regional *SOX3* expression are located across at least a 500-kb interval flanking the gene, it is plausible that these rearrangements activate *SOX3* expression in the gonad, perhaps by generating a gonadal enhancer or ablation of a repression element (62). Indeed, the centromeric duplication breakpoint in patients A and C is in close proximity to a previously described deletion-insertion breakpoint in individuals with X-linked hypoparathyroidism, which was proposed to induce ectopic *SOX3* expression (61). While it would be very interesting to assess the impact of *SOX3* rearrangements on embryonic gonadal expression in humans, this is obviously not possible. However, based on our analysis of the *Sr* transgenic mice, these are exactly the kind of mutations that could reasonably be expected to occur in patients with XX male sex reversal. Notably, *SOX3* expression was not detected in a lymphoblast cell line from patient B (the only patient from whom a cell line was available; data not shown), suggesting that the rearrangement has not caused widespread ectopic *SOX3* expression, which instead may be relatively restricted and include the developing gonad.

Taken together, these data provide a molecular entry point into the etiology of XX male sex reversal in humans. It is worth noting the high frequency of *SOX3* rearrangements in 46, XX male patients (19%), suggesting that this may be a significant cause of this disorder. Indeed, this may be an underestimate given that balanced rearrangements/translocations would not have been detected by our analysis. Further chromosomal and molecular analysis of DSD patient cohorts is therefore required to determine the relative contribution of *SOX3* rearrangements to the underlying pathology of this poorly understood group of conditions.

Methods

Generation of Sr transgenic mice. The transgene construct was derived from a modified BAC clone (RP23-174O19) containing an internal ribosome entry site–EGFP (IRES-EGFP) reporter cassette inserted into the 3′UTR of *Sox3* using homologous recombination (83). The PCR product for recombineering contained a 5′ *Sox3* homology arm, IRES-EGFP reporter, FRT site, kanamycin resistance cassette, FRT site, and 3′ *Sox3* homology arm and was generated using Expand High Fidelity PCR System (Roche) amplification of a modified pIRES2-EGFP plasmid (BD Biosciences — Clontech; forward primer: **CAGCTCTTCGCCCCCACCCCGCCCCACACCCCCCAC-GTTGGGACGCCTTG**GCCCCTCTCCCTCCCCCCCCCCTAA; Reverse primer: **CGCACTTCAAATTTCGGACCCGCAAAATTATCAGGACTC-CAGCATATTGG***GAAGTTCCTATTCTCTAGAAAGTATAGGAACTTC*ATT-TATTCTGTCTTTTTATTGCCGTC (*Sox3* homology sequence is in bold and FRT site in italics). The kanamycin resistance cassette was removed in bacteria prior to transgene preparation using an FLP recombinase expression vector. The 37-kb transgene spanned positions 58,136,727–58,172,890 of the X chromosome (July 2007 [NCBI 39/mm9] assembly) and contained approximately 26 kb and 8 kb of 5′ and 3′ *Sox3* genomic sequence, respectively. It was generated by *Pme*I/*Ahd*I digestion, purified by agarose gel electrophoresis and microdialysis, and injected into the pronucleus of C57BL/6 × CBA F_1 zygotes. The *Sr* line was established from an XY founder animal and was maintained on a C57BL/6 × CBA mixed genetic background. Routine genotyping was performed by PCR amplification of genomic DNA derived from tail biopsies (weanlings) or embryonic/yolk sac tissue (embryos) using PCR (*Sry* primers: CACTGGCCTTTTCTCCTACC and CATGGCATGCTGTATTGACC; *Gapdh* primers: CTTGCTCAGTGTCCTTGCTG and ACCCAGAAGACTGT-GGATGG; *Egfp*: ATGGTGAGCAAGGGCGAGGAGCTGTT and CTGGGT-GCTCAGGTAGTGGTTGTC; cycle conditions: denaturation 95°C 2 minutes; amplification 95°C 30 seconds, 60°C 30 seconds, 72°C 3 minutes 30 seconds (35 cycles); final extension 72°C 7 minutes, 25°C 5 minutes). For the *Sox9* rescue experiment, previously published lines that contain a homozygous floxed allele of *Sox9* (*Sox9*$^{fl/fl}$) (84) and a tamoxifen-inducible CreERT2 knocked into the Rosa26 locus (R26-CreERT2) (85) maintained on a F_1 (C57BL/10 × CBA) genetic background were used. Tamoxifen (Sigma-Aldrich) was dissolved in ethanol at 100 mg/ml. To activate Cre-ERT2, the tamoxifen solution was diluted with sunflower oil to the final concentration of 10 mg/ml, and 0.3 ml of the diluted solution was administered by gavage to pregnant mice at 9.5 and 10.5 dpc. All animal experimentation was performed in accordance with the *Australian Code of Practice for the Care and Use of Animals for Scientific Purposes* and was approved by the University of Adelaide Animal Ethics Committee or by the UK Home Office.

FISH of chromosomes. For mouse studies, FISH probes were directly labeled with spectrum orange/spectrum green using commercial kits (Vysis). Hybridization to metaphase spreads and fluorescence detection were performed on metaphase preparations as previously described (86). For human studies, FISH using BAC RP11-51C14 was carried out on metaphase spreads obtained from the 46, XX male patient according to previously described methods (87).

Cloning the Sr integration site. The 5′ integration site was identified by GenomeWalker (BD Biosciences — Clontech) amplification of Tg/+ genomic DNA using nested *Sox3* transgene primers (Sox3GSP1: ACAGCCTT-GTGAGTAGGTATGCTCTTG; Sox3GSP2: CTTCTTTGTGCGGACCCT-TATTCCAAG). The sequence immediately 5′ to the transgene integration site was identified as a long interspersed nuclear element (LINE) repeat using RepeatMasker (http://www.repeatmasker.org/) and could not be unequivocally assigned to a genomic location using BLAST (http://www.ncbi.nlm.nih.gov/) or BLAT (http://genome.ucsc.edu/) analysis. However, a LINE repeat that perfectly matched this transgene-flanking sequence was identified by megaBLAST analysis of the mouse genome sequence trace

archive (http://www.ncbi.nlm.nih.gov/blast/mmtrace.shtml), and a contig was assembled through reiterative interrogation. PCR amplification using unique flanking sequence and transgene primers generated a product from Tg/+ genomic DNA and not +/+ genomic DNA (primers: ACAGCCTTGTGAGTAGGTATGCTCTTG and TGGCTGTGGTAACCATTCATAAGGTAG; cycle conditions: denaturation 95°C 2 minutes; amplification 95°C 30 seconds, 60°C 30 seconds, 72°C 3 minutes [35 cycles]; final extension 72°C 7 minutes, 25°C 5 minutes). Sequencing confirmed the authenticity of this PCR product. To further confirm the integration site of the *Sr* transgene, standard Southern blot analysis was performed using a ^{32}P-labeled chromosome 19–specific probe that spanned positions 20547495–20548089 (July 2007 assembly).

Immunohistochemistry, histology, and imaging. Mouse embryos were dissected in PBS, fixed in 4% PFA/PBS, cryoprotected in 30% sucrose, and embedded in OCT medium. Sections (10 μm) were prepared using a Leica CM1900 cryostat. Blocking in PBS/0.1% Triton X-100/1% BSA/10% heat-inactivated horse serum was performed for 30 minutes, followed by overnight incubation at 4°C in the same solution containing diluted primary antibody. Sections were washed 3 times for 10 minutes in PBS and incubated in diluted secondary antibody at 4°C for 6 hours. After washing 3 times for 10 minutes each in PBS, slides were mounted in Prolong Gold Antifade (Molecular Probes, Invitrogen) and imaged using a Zeiss Axioplan 2 microscope and AxioCam MRm with Axiovision software. Antibodies and their corresponding dilutions were: rabbit anti-ALDH1A1 (Abcam Ab24343; 1:200), goat anti-SOX3 (R&D Systems; 1:100), rabbit anti-EGFP (Abcam; 1:2,000), goat anti-EGFP (Rockland; 1:400), rabbit anti-SOX9 (19) (1:1,000), goat anti-SOX9 (R&D Systems; 1:300), rabbit anti-FOXL2 (gift from Dagmar Wilhelm, Institute for Molecular Bioscience, The University of Queensland, Brisbane, Queensland, Australia; 1:1,000), Cy3–donkey anti-rabbit (Jackson ImmunoResearch Laboratories Inc.; 1:400), Cy5–donkey anti-goat (Jackson ImmunoResearch Laboratories Inc.; 1:400), Cy3–donkey anti-rabbit (Rockland; 1:1,000), Cy3–donkey anti-goat (Jackson ImmunoResearch Laboratories Inc.; 1:400) and Cy5–donkey anti-rabbit (Jackson ImmunoResearch Laboratories Inc.; 1:400) and Alexa Fluor 488–donkey anti-goat (Molecular Probes, Invitrogen; 1:400). Adult testis were fixed in Bouin's fixative and stained using hematoxylin and eosin. Whole mount images were captured using a Nikon SMZ1000 GFP dissecting microscope with AnalySIS software and processed using Adobe Photoshop CS. Confocal images were captured on a Leica Sp5 Spectral scanning confocal microscope and processed using Leica Application Suite — Advanced Fluorescence 1.8.0 build 1346. Select images were subject to median measurements using a radius of 3 with 4 iterations to decrease graininess from the Cy5 fluorophore.

Whole mount and section in situ hybridization. Whole mount in situ hybridization and in situ hybridization of 10-μm cryosections were performed as described previously (88, 89). The *Aldh1a1* plasmid was a gift from Peter Koopman (Institute for Molecular Bioscience, The University of Queensland). The *Sox9* and *Amh* plasmids were published previously (19, 90).

RNA extraction and qRT-PCR analysis. RNA extractions were performed on GR explants and contained mesonephros unless stated otherwise. For 10.5- and 11.5-dpc embryos, the two genital ridges were pooled from each embryo, while individual gonads and associated mesonephros were isolated from 12.5-dpc and 13.5-dpc embryos. Samples were homogenized by brief sonication prior to being passed over QIAshredder columns (QIAGEN). RNA was isolated using the RNeasy Plus kit (QIAGEN) and analyzed for RNA integrity and concentration on a Bioanalyzer (Agilent). Fifty nanograms of each sample was reverse transcribed using the High Capacity RNA-to-cDNA kit (Applied Biosystems). qRT-PCR was performed using Fast SYBR Green Master Mix (Applied Biosystems) and run on an ABI 7500 StepOnePlus system. Gene-specific primer pairs were designed to cross intron-exon boundaries. The sequences and lengths of amplified products were: *Aldh1a1* (158 bp) 5′-CCTTGCATTGTGTTTGCAGATG-3′ and 5′-GCTCGCTCAACACTCCTTTTC-3′; *Sox9* (106 bp) 5′-GCAAGCTGGCAAAGTTGATCT-3′ and 5′-GCTGCTCAGTTCACCGATG-3′; *EGFP* (95 bp) 5′-ACGACGGCAACTACAAGACC-3′ and 5′-GTCCTCCTTGAAGTCGATGC-3′; and β-*actin* (89 bp) 5′-CTGCCTGACGGCCAGG-3′ and 5′-GATTCCATACCCAAGAAGGAAGG-3′. Efficiency of the amplification was verified by analysis of standard curves. No template and minus-RT controls were performed to ensure signal was cDNA-specific.

Cotransfection assays. Transactivation assays using the mouse TESCO reporter were performed in COS7 cells as described previously (18). DNA encoding human SRY, SF1, and mouse and human SOX3 were contained within the pcDNA3 mammalian expression plasmid (Clontech). The *hTES* sequence was amplified from the BAC contig clone RP11-84E24 (GenBank AC007461), located on chromosome 17, by PCR using a forward oligonucleotide containing an *Xho*I restriction site (GATCATCCGCTCGAGCGGTGTTGAGAAGTGAACTGT) and a reverse oligonucleotide containing an *Acc*I restriction site (GATGGCCGGTCGACCGGCCACTTGGCTCAAATCTCAC). The resultant PCR product was cloned into the multiple cloning site of the E1b-*luc* reporter construct (91). hTES cotransfection assays were conducted in the CHO cell line cultured in Dulbecco's medium supplemented with 10% fetal bovine serum and L-glutamine in an atmosphere of 5% CO_2. Briefly, cells were seeded at a density of 2.3×10^5 cells per well in a 6-well plate 24 hours prior to transfection. Forty-eight hours after transfection, the culture media was removed, cell lysate collected, and luciferase reporter activity measured according to the manufacturer's instructions (Promega). Reporter activity was normalized to β-*galactosidase* as an internal control (Promega). Empty reporter, E1b-*luc*, transfection data were subtracted from each transfection condition to standardize data. Fold activations were determined by dividing by vector-alone transfection data.

Microarray analysis. Genomic DNA from patients A and B was hybridized to an Affymetrix Genome-Wide Human SNP 6.0 array at the Australian Genome Research Facility according to the manufacturer's instructions. Data analysis was performed with An R Object-oriented Microarray Analysis (AROMA) algorithm (92). Multiplex ligation–dependent probe amplification (MLPA) analysis to confirm the duplication was performed as previously described (93). Genomic DNA from patient C was hybridized to an Illumina Human1M-Duo DNA Analysis BeadChip at the Southern California Genotyping Consortium according to the manufacturer's instructions. Data analysis was performed using CNV partition v2.3.4 on Illumina Genome Studio (94).

Clinical data. Clinical data for patients A, B, and C are summarized in Table 1. These studies were approved by the Human Research Ethics Committee of the Royal Children's Hospital, Melbourne, and the UCLA Institutional Review Board. Written informed consent was obtained from participants or their parents/guardians.

Patient A is a male of European descent who presented at 30 years of age for infertility. He had no significant past medical history and was healthy at time of presentation. His height was 165 cm, and he weighed 64 kg, with no abnormal symptoms. He underwent puberty between 14 and 15 years of age. Family history was not significant, and there was no consanguinity. Infertility was indicated by two spermograms, which confirmed azoospermia. Testicular biopsy was not performed. The patient was *SRY*-negative (data not shown). Parental DNA was not available.

Patient B is a 35-year-old of European descent. Gender dysphoria was reported from around 6 years, leading ultimately to gender reassignment surgery at age 26 years. Puberty commenced around age 14. At age 19, height was 167.5 cm, weight 73.5 kg, with no medical problems apart from ongoing gender identity issues. The external genitalia were normal male, apart from small, soft 6-ml testes (by orchidometer), subsequently measured at less than 4 ml (by orchidometer) at age 25 years. Shaving was infrequent, and there was little body hair, but axillary and pubic hair was normal (minimal abdominal extension). Primary hypogonadism was evident

at age 19 years, with follicle-stimulating hormone (FSH) and luteinizing hormone (LH) both elevated, at 69 mIU/ml and 35 mIU/ml, respectively, and random free testosterone level being low, at 8.7 pg/ml. Serum prolactin was normal. Histological examination following gender reassignment surgery showed atrophic changes in the testes, with loss of normal spermatogenesis, thickening and hyalinization of the tubular basal lamina, and diminished number of interstitial cells. Spermatic cords were histologically normal, as was the penis. The patient was SRY-negative in both peripheral blood and testicular tissue. The *SOX3* rearrangement was not present in his mother. DNA was not available for the father.

Patient C is a boy of Mexican origin who presented at 19 months with failure to thrive and developmental delay (height 75.2 cm [<5th percentile]). There were no significant problems during pregnancy or the newborn period, and cytogenetic analysis showed that this child was 46, XX, *SRY*-negative. Family history was significant only for learning disabilities. There was no consanguinity. No endocrine evaluation or parental DNA was available.

Statistics. Statistical analysis for transactivation assays was conducted using a 2-tailed, paired Student's *t* test, and $P < 0.05$ was considered significant. Error bars indicate the mean ± SEM in Figure 4 and SD in Figure 10.

Acknowledgments

The authors thank Peter Koopman and Josephine Bowles for sharing unpublished data and useful discussions, Terry Speed for assistance with microarray analysis, and Frank Grutzner for critical reading of the manuscript. We also thank Sandra Piltz, Mizuho Mamiya, Rhonda Hutchinson, Julie Scott, and the staff of the University of Adelaide Laboratory Animal Services for technical assistance. The authors also thank Tiago Rocha for patient A's clinical evaluation and the staff of Unidade de Citogenética of Instituto Nacional de Saúde Ricardo Jorge for the chromosome analysis, as well as the contribution of the patients involved in the study. We gratefully acknowledge funding support from the Australian Research Council (P. Thomas), the Australian National Health and Medical Research Council (P. Thomas, S. White, A. Sinclair, and V. Harley), the UK Medical Research Council (U117512772) (R. Lovell-Badge), the Helen Macpherson Smith Trust (A. Sinclair), the Fundação para a Ciência e a Tecnologia (FCT; POCTI/SAU/97/2001) and the Centro de Investigação em Genética Molecular Humana da Universidade Nova de Lisboa (J. Goncalves), the Doris Duke Charitable Foundation (E. Vilain), and the Louis Jeantet Foundation (R. Lovell-Badge). Paul Thomas is a Pfizer Australia Research Fellow.

Received for publication February 8, 2010, and accepted in revised form October 27, 2010.

Address correspondence to: Paul Thomas, Level 3, Molecular Life Sciences Building, University of Adelaide, North Terrace, Adelaide, South Australia, 5005 Australia. Phone: 61.8.8303.7047; Fax: 61.8.8303.4362; E-mail: paul.thomas@adelaide.edu.au.

1. Blackless M, et al. How sexually dimorphic are we? Review and synthesis. *Am J Hum Biol*. 2000; 12(2):151–166.
2. Temel SG, et al. Extended pedigree with multiple cases of XX sex reversal in the absence of SRY and of a mutation at the SOX9 locus. *Sex Dev*. 2007;1(1):24–34.
3. Sinclair AH, et al. A gene from the human sex-determining region encodes a protein with homology to a conserved DNA-binding motif. *Nature*. 1990;346(6281):240–244.
4. Lovell-Badge R, Robertson E. XY female mice resulting from a heritable mutation in the primary testis-determining gene, Tdy. *Development*. 1990;109(3):635–646.
5. Lim HN, Berkovitz GD, Hughes IA, Hawkins JR. Mutation analysis of subjects with 46, XX sex reversal and 46, XY gonadal dysgenesis does not support the involvement of SOX3 in testis determination. *Hum Genet*. 2000;107(6):650–652.
6. Koopman P, Munsterberg A, Capel B, Vivian N, Lovell-Badge R. Expression of a candidate sex-determining gene during mouse testis differentiation. *Nature*. 1990;348(6300):450–452.
7. Koopman P, Gubbay J, Vivian N, Goodfellow P, Lovell-Badge R. Male development of chromosomally female mice transgenic for Sry. *Nature*. 1991;351(6322):117–121.
8. Gubbay J, et al. A gene mapping to the sex-determining region of the mouse Y chromosome is a member of a novel family of embryonically expressed genes. *Nature*. 1990;346(6281):245–250.
9. Just W, et al. Absence of Sry in species of the vole Ellobius. *Nat Genet*. 1995;11(2):117–118.
10. Soullier S, Hanni C, Catzeflis F, Berta P, Laudet V. Male sex determination in the spiny rat Tokudaia osimensis (Rodentia: Muridae) is not Sry dependent. *Mamm Genome*. 1998;9(7):590–592.
11. Waters PD, Wallis MC, Marshall Graves JA. Mammalian sex — origin and evolution of the Y chromosome and SRY. *Semin Cell Dev Biol*. 2007;18(3):389–400.
12. Albrecht KH, Eicher EM. Evidence that Sry is expressed in pre-Sertoli cells and Sertoli and granulosa cells have a common precursor. *Dev Biol*. 2001;240(1):92–107.
13. Hacker A, Capel B, Goodfellow P, Lovell-Badge R. Expression of Sry, the mouse sex determining gene. *Development*. 1995;121(6):1603–1614.
14. Bullejos M, Koopman P. Spatially dynamic expression of Sry in mouse genital ridges. *Dev Dyn*. 2001;221(2):201–205.
15. Nagamine CM, Morohashi K, Carlisle C, Chang DK. Sex reversal caused by Mus musculus domesticus Y chromosomes linked to variant expression of the testis-determining gene Sry. *Dev Biol*. 1999;216(1):182–194.
16. Hiramatsu R, et al. A critical time window of Sry action in gonadal sex determination in mice. *Development*. 2009;136(1):129–138.
17. Bullejos M, Koopman P. Delayed Sry and Sox9 expression in developing mouse gonads underlies B6-Y(DOM) sex reversal. *Dev Biol*. 2005;278(2):473–481.
18. Sekido R, Lovell-Badge R. Sex determination involves synergistic action of SRY and SF1 on a specific Sox9 enhancer. *Nature*. 2008;453(7197):930–934.
19. Sekido R, Bar I, Narvaez V, Penny G, Lovell-Badge R. SOX9 is up-regulated by the transient expression of SRY specifically in Sertoli cell precursors. *Dev Biol*. 2004;274(2):271–279.
20. Palmer SJ, Burgoyne PS. In situ analysis of fetal, prepuberal and adult XX----XY chimaeric mouse testes: Sertoli cells are predominantly, but not exclusively, XY. *Development*. 1991;112(1):265–268.
21. Wilhelm D, et al. Sertoli cell differentiation is induced both cell-autonomously and through prostaglandin signaling during mammalian sex determination. *Dev Biol*. 2005;287(1):111–124.
22. Kim Y, et al. Fgf9 and Wnt4 act as antagonistic signals to regulate mammalian sex determination. *PLoS Biol*. 2006;4(6):e187.
23. Capel B, Albrecht KH, Washburn LL, Eicher EM. Migration of mesonephric cells into the mammalian gonad depends on Sry. *Mech Dev*. 1999; 84(1–2):127–131.
24. DiNapoli L, Capel B. SRY and the standoff in sex determination. *Mol Endocrinol*. 2008;22(1):1–9.
25. Tomizuka K, et al. R-spondin1 plays an essential role in ovarian development through positively regulating Wnt-4 signaling. *Hum Mol Genet*. 2008;17(9):1278–1291.
26. Parma P, et al. R-spondin1 is essential in sex determination, skin differentiation and malignancy. *Nat Genet*. 2006;38(11):1304–1309.
27. Maatouk DM, DiNapoli L, Alvers A, Parker KL, Taketo MM, Capel B. Stabilization of beta-catenin in XY gonads causes male-to-female sex-reversal. *Hum Mol Genet*. 2008;17(19):2949–2955.
28. Jeays-Ward K, et al. Endothelial and steroidogenic cell migration are regulated by WNT4 in the developing mammalian gonad. *Development*. 2003; 130(16):3663–3670.
29. Chang H, Gao F, Guillou F, Taketo MM, Huff V, Behringer RR. Wt1 negatively regulates beta-catenin signaling during testis development. *Development*. 2008;135(10):1875–1885.
30. Jordan BK, Shen JH, Olaso R, Ingraham HA, Vilain E. Wnt4 overexpression disrupts normal testicular vasculature and inhibits testosterone synthesis by repressing steroidogenic factor 1/beta-catenin synergy. *Proc Natl Acad Sci U S A*. 2003;100(19):10866–10871.
31. Stevanovic M, Lovell-Badge R, Collignon J, Goodfellow PN. SOX3 is an X-linked gene related to SRY. *Hum Mol Genet*. 1993;2(12):2013–2018.
32. Foster JW, Graves JA. An SRY-related sequence on the marsupial X chromosome: implications for the evolution of the mammalian testis-determining gene. *Proc Natl Acad Sci U S A*. 1994;91(5):1927–1931.
33. Collignon J, et al. A comparison of the properties of Sox-3 with Sry and two related genes, Sox-1 and Sox-2. *Development*. 1996;122(2):509–520.
34. Wallis MC, Waters PD, Graves JA. Sex determination in mammals — before and after the evolution of SRY. *Cell Mol Life Sci*. 2008;65(20):3182–3195.
35. Bowles J, Schepers G, Koopman P. Phylogeny of the SOX family of developmental transcription factors based on sequence and structural indicators. *Dev Biol*. 2000;227(2):239–255.
36. Graves JA. Sex chromosome specialization and degeneration in mammals. *Cell*. 2006;124(5):901–914.
37. Pask AJ, Harry JL, Renfree MB, Marshall Graves JA. Absence of SOX3 in the developing marsupial gonad is not consistent with a conserved role in mammali-

an sex determination. *Genesis*. 2000;27(4):145–152.
38. Woods KS, et al. Over- and underdosage of SOX3 is associated with infundibular hypoplasia and hypopituitarism. *Am J Hum Genet*. 2005;76(5):833–849.
39. Solomon NM, et al. Array comparative genomic hybridisation analysis of boys with X linked hypopituitarism identifies a 3.9 Mb duplicated critical region at Xq27 containing SOX3. *J Med Genet*. 2004;41(9):669–678.
40. Rizzoti K, Brunelli S, Carmignac D, Thomas PQ, Robinson IC, Lovell-Badge R. SOX3 is required during the formation of the hypothalamo-pituitary axis. *Nat Genet*. 2004;36(3):247–255.
41. Laumonnier F, et al. Transcription factor SOX3 is involved in X-linked mental retardation with growth hormone deficiency. *Am J Hum Genet*. 2002;71(6):1450–1455.
42. Dee CT, Hirst CS, Shih YH, Tripathi VB, Patient RK, Scotting PJ. Sox3 regulates both neural fate and differentiation in the zebrafish ectoderm. *Dev Biol*. 2008;320(1):289–301.
43. Bylund M, Andersson E, Novitch BG, Muhr J. Vertebrate neurogenesis is counteracted by Sox1-3 activity. *Nat Neurosci*. 2003;6(11):1162–1168.
44. Rizzoti K, Lovell-Badge R. SOX3 activity during pharyngeal segmentation is required for craniofacial morphogenesis. *Development*. 2007;134(19):3437–3448.
45. Weiss J, Meeks JJ, Hurley L, Raverot G, Frassetto A, Jameson JL. Sox3 is required for gonadal function, but not sex determination, in males and females. *Mol Cell Biol*. 2003;23(22):8084–8091.
46. Raverot G, Weiss J, Park SY, Hurley L, Jameson JL. Sox3 expression in undifferentiated spermatogonia is required for the progression of spermatogenesis. *Dev Biol*. 2005;283(1):215–225.
47. Solomon NM, Nouri S, Warne GL, Lagerstrom-Fermer M, Forrest SM, Thomas PQ. Increased gene dosage at Xq26-q27 is associated with X-linked hypopituitarism. *Genomics*. 2002;79(4):553–559.
48. De Santa Barbara P, et al. Direct interaction of SRY-related protein SOX9 and steroidogenic factor 1 regulates transcription of the human anti-Mullerian hormone gene. *Mol Cell Biol*. 1998;18(11):6653–6665.
49. Hiramatsu R, et al. Regionally distinct potencies of mouse XY genital ridge to initiate testis differentiation dependent on anteroposterior axis. *Dev Dyn*. 2003;228(2):247–253.
50. Bagheri-Fam S, et al. Loss of Fgfr2 leads to partial XY sex reversal. *Dev Biol*. 2008;314(1):71–83.
51. Huang B, Wang S, Ning Y, Lamb AN, Bartley J. Autosomal XX sex reversal caused by duplication of SOX9. *Am J Med Genet*. 1999;87(4):349–353.
52. Qin Y, Kong LK, Poirier C, Truong C, Overbeek PA, Bishop CE. Long-range activation of Sox9 in Odd Sex (Ods) mice. *Hum Mol Genet*. 2004;13(12):1213–1218.
53. Sekido R, Lovell-Badge R. Sex determination and SRY: down to a wink and a nudge? *Trends Genet*. 2009;25(1):19–29.
54. Canning CA, Lovell-Badge R. Sry and sex determination: how lazy can it be? *Trends Genet*. 2002; 18(3):111–113.
55. Vasiliou V, Pappa A, Estey T. Role of human aldehyde dehydrogenases in endobiotic and xenobiotic metabolism. *Drug Metab Rev*. 2004;36(2):279–299.
56. Duester G, Mic FA, Molotkov A. Cytosolic retinoid dehydrogenases govern ubiquitous metabolism of retinol to retinaldehyde followed by tissue–specific metabolism to retinoic acid. *Chem Biol Interact*. 2003;143–144:201–210.
57. Fan X, et al. Targeted disruption of Aldh1a1 (Raldh1) provides evidence for a complex mechanism of retinoic acid synthesis in the developing retina. *Mol Cell Biol*. 2003;23(13):4637–4648.
58. Matt N, et al. Retinoic acid-dependent eye morphogenesis is orchestrated by neural crest cells. *Development*. 2005;132(21):4789–4800.
59. McClive PJ, Hurley TM, Sarraj MA, van den Bergen JA, Sinclair AH. Subtractive hybridisation screen identifies sexually dimorphic gene expression in the embryonic mouse gonad. *Genesis*. 2003;37(2):84–90.
60. Bowles J, et al. Male-specific expression of Aldh1a1 in mouse and chicken fetal testes: implications for retinoid balance in gonad development. *Dev Dyn*. 2009;238(8):2073–2080.
61. Bowl MR, et al. An interstitial deletion-insertion involving chromosomes 2p25.3 and Xq27.1, near SOX3, causes X-linked recessive hypoparathyroidism. *J Clin Invest*. 2005;115(10):2822–2831.
62. Navratilova P, Fredman D, Hawkins TA, Turner K, Lenhard B, Becker TS. Systematic human/zebrafish comparative identification of cis-regulatory activity around vertebrate developmental transcription factor genes. *Dev Biol*. 2009;327(2):526–540.
63. Bagheri-Fam S, Sinclair AH, Koopman P, Harley VR. Conserved regulatory modules in the Sox9 testis-specific enhancer predict roles for SOX, TCF/LEF, Forkhead, DMRT, and GATA proteins in vertebrate sex determination. *Int J Biochem Cell Biol*. 2010;42(3):472–477.
64. Polanco JC, Koopman P. Sry and the hesitant beginnings of male development. *Dev Biol*. 2007; 302(1):13–24.
65. Kidokoro T, et al. Influence on spatiotemporal patterns of a male-specific Sox9 activation by ectopic Sry expression during early phases of testis differentiation in mice. *Dev Biol*. 2005;278(2):511–525.
66. Lee CH, Taketo T. Normal onset, but prolonged expression, of Sry gene in the B6.YDOM sex-reversed mouse gonad. *Dev Biol*. 1994;165(2):442–452.
67. Chaboissier MC, et al. Functional analysis of Sox8 and Sox9 during sex determination in the mouse. *Development*. 2004;131(9):1891–1901.
68. Hanley NA, et al. SRY, SOX9, and DAX1 expression patterns during human sex determination and gonadal development. *Mech Dev*. 2000;91(1–2):403–407.
69. Taketo T, Lee CH, Zhang J, Li Y, Lee CY, Lau YF. Expression of SRY proteins in both normal and sex-reversed XY fetal mouse gonads. *Dev Dyn*. 2005;233(2):612–622.
70. Palmer SJ, Burgoyne PS. The Mus musculus domesticus Tdy allele acts later than the Mus musculus musculus Tdy allele: a basis for XY sex-reversal in C57BL/6-YPOS mice. *Development*. 1991;113(2):709–714.
71. Lee CH, Taketo T. Low levels of Sry transcripts cannot be the sole cause of B6-Y(TIR) sex reversal. *Genesis*. 2001;30(1):7–11.
72. Albrecht KH, Young M, Washburn LL, Eicher EM. Sry expression level and protein isoform differences play a role in abnormal testis development in C57BL/6J mice carrying certain Sry alleles. *Genetics*. 2003;164(1):277–288.
73. Munger SC, Aylor DL, Syed HA, Magwene PM, Threadgill DW, Capel B. Elucidation of the transcription network governing mammalian sex determination by exploiting strain-specific susceptibility to sex reversal. *Genes Dev*. 2009;23(21):2521–2536.
74. Bergstrom DE, Young M, Albrecht KH, Eicher EM. Related function of mouse SOX3, SOX9, and SRY HMG domains assayed by male sex determination. *Genesis*. 2000;28(3–4):111–124.
75. Lovell-Badge R, Canning C, Sekido R. Sex–determining genes in mice: building pathways. *Novartis Found Symp*. 2002;244:4–18; discussion 18–22, 35–42, and 253–257.
76. Graves JA. Interactions between SRY and SOX genes in mammalian sex determination. *Bioessays*. 1998;20(3):264–269.
77. Dewing P, et al. Direct regulation of adult brain function by the male-specific factor SRY. *Curr Biol*. 2006;16(4):415–420.
78. Mayer A, Lahr G, Swaab DF, Pilgrim C, Reisert I. The Y-chromosomal genes SRY and ZFY are transcribed in adult human brain. *Neurogenetics*. 1998;1(4):281–288.
79. Milsted A, Serova L, Sabban EL, Dunphy G, Turner ME, Ely DL. Regulation of tyrosine hydroxylase gene transcription by Sry. *Neurosci Lett*. 2004;369(3):203–207.
80. Vidal VP, Chaboissier MC, de Rooij DG, Schedl A. Sox9 induces testis development in XX transgenic mice. *Nat Genet*. 2001;28(3):216–217.
81. Polanco JC, Wilhelm D, Davidson TL, Knight D, Koopman P. Sox10 gain-of-function causes XX sex reversal in mice: implications for human 22q-linked disorders of sex development. *Hum Mol Genet*. 2010;19(3):506–516.
82. Lin L, et al. Heterozygous missense mutations in steroidogenic factor 1 (SF1/Ad4BP, NR5A1) are associated with 46,XY disorders of sex development with normal adrenal function. *J Clin Endocrinol Metab*. 2007;92(3):991–999.
83. Lee EC, et al. A highly efficient Escherichia coli-based chromosome engineering system adapted for recombinogenic targeting and subcloning of BAC DNA. *Genomics*. 2001;73(1):56–65.
84. Akiyama H, Chaboissier M C, Martin J F, Schedl A, de Crombrugghe B. The transcription factor Sox9 has essential roles in successive steps of the chondrocyte differentiation pathway and is required for expression of Sox5 and Sox6. *Genes Dev*. 2002;16(21):2813–2828.
85. Seibler J, et al. Rapid generation of inducible mouse mutants. *Nucleic Acids Res*. 2003;31(4):e12.
86. Baker E, et al. Study of 250 children with idiopathic mental retardation reveals nine cryptic and diverse subtelomeric chromosome anomalies. *Am J Med Genet*. 2002;107(4):285–293.
87. Bruno DL, et al. Detection of cryptic pathogenic copy number variations and constitutional loss of heterozygosity using high resolution SNP microarray analysis in 117 patients referred for cytogenetic analysis and impact on clinical practice. *J Med Genet*. 2009;46(2):123–131.
88. Thomas PQ, Brown A, Beddington RS. Hex: a homeobox gene revealing peri-implantation asymmetry in the mouse embryo and an early transient marker of endothelial cell precursors. *Development*. 1998;125(1):85–94.
89. Wilson LD, Ross SA, Lepore DA, Wada T, Penninger JM, Thomas PQ. Developmentally regulated expression of the regulator of G-protein signaling gene 2 (Rgs2) in the embryonic mouse pituitary. *Gene Expr Patterns*. 2005;5(3):305–311.
90. Swain A, Narvaez V, Burgoyne P, Camerino G, Lovell-Badge R. Dax1 antagonizes Sry action in mammalian sex determination. *Nature*. 1998;391(6669):761–767.
91. Bernard P, Fleming A, Lacombe A, Harley VR, Vilain E. Wnt4 inhibits beta-catenin/TCF signalling by redirecting beta-catenin to the cell membrane. *Biol Cell*. 2008;100(3):167–177.
92. Bengtsson H, Irizarry R, Carvalho B, Speed TP. Estimation and assessment of raw copy numbers at the single locus level. *Bioinformatics*. 2008;24(6):759–767.
93. White SJ, et al. Two-color multiplex ligation-dependent probe amplification: detecting genomic rearrangements in hereditary multiple exostoses. *Hum Mutat*. 2004;24(1):86–92.
94. Yau C, Holmes CC. CNV discovery using SNP genotyping arrays. *Cytogenet Genome Res*. 2008; 123(1–4):307–312.
95. Journal of the American Medical Association. Système International (SI) Conversion Factors for Selected Laboratory Components. http://jama.ama.assn.org/content/vol295/issue1/images/data/103/DC6/JAMA_auinst_si.dtl#dual. Updated September 28, 2001.
96. Rosner W, Auchus RJ, Azziz R, Sluss PM, Raff H. Position statement: utility, limitations, and pitfalls in measuring testosterone: an Endocrine Society position statement. *J Clin Endocrinol Metab*. 2007;92(2):405–413.